5-2007

Photopolymerization-Induced Directional Crystal Growth in Reactive Mixtures

Soo Jeoung Park
University of Akron Main Campus

Pankaj Rathi
University of Akron Main Campus

Thein Kyu
University of Akron Main Campus, tkyu@uakron.edu

Photopolymerization-induced directional crystal growth in reactive mixtures

Soo Jeoung Park, Pankaj Rathi, and Thein Kyu*
Department of Polymer Engineering, University of Akron, Akron, Ohio 44325, USA
(Received 22 August 2006; published 30 May 2007)

Photopolymerization-induced crystallization has been demonstrated in blends of polyethylene oxide–diacrylate at temperatures above the depressed melting temperature of the crystalline component. Upon exposure to ultraviolet irradiation, the melting transition curve moves upward and eventually surpasses the reaction temperature, thereby inducing phase separation as well as crystallization. The present paper demonstrates the occurrence of directionally solidified interface morphologies of polymer crystals subjected to a photointensity gradient. The epitaxially grown seaweed or degenerate structures were observed at the circumference (low-intensity region) while the dense branched spherulites developed at the core high-intensity region.

DOI: 10.1103/PhysRevE.75.051804 PACS number(s): 61.41.+e, 64.60.Cn, 64.75.+g

I. INTRODUCTION

The photopolymerization-induced phase transition is the phenomenon of nonequilibrium phase transformation involving liquid-liquid phase separation, crystallization, and/or mesophase ordering from an isotropic liquid (or melt) driven by a photochemical reaction [1,2]. During the course of photopolymerization of the reactive monomer, the average molecular weight of the reactive constituent in the polymer blends increases, which in turn makes the system become unstable and eventually drives phase segregation [1–5]. In crystalline or liquid crystalline polymer mixtures, liquid-liquid phase separation occurs in competition with crystal solidification or mesophase ordering during photopolymerization [6–9]. The phenomenon of photopolymerization-induced crystallization bears some resemblance to crystallization in thermally quenched blends that occurs in competition with liquid-liquid phase separation [10–13]. However, it should be noted that, even though the reaction is usually carried out at a constant temperature, supercooling increases with progress of the reaction, and thus the crystallization process during photopolymerization is analogous to nonisothermal gradual cooling.

The primary objective of the present study is directed to elucidation of directional phase transitions, such as oriented crystallization induced by a photointensity gradient during photopolymerization of a crystalline polymer–photocurable monomer mixture. The concept of polymerization-induced crystallization is similar to that of liquid-liquid phase separation in binary polymer blends undergoing a thermally initiated cross-linking reaction or photochemically initiated polymerization [6,7]. While the polymerization-induced phase separation has been well investigated experimentally and theoretically [1–9], the phenomenon of polymerization-induced crystallization has virtually been overlooked. In addition, the polymerization-driven phase transition in soft materials such as crystal or liquid crystal mixtures shares some common ground with the directional solidification of conventional materials such as metal alloys or ceramic mixtures [14–21] and excitable media such as biological systems [22].

*Electronic address: tkyu@uakron.edu

II. MATERIALS AND EXPERIMENT

In the present paper, the melting point depression of polyethylene oxide (PEO) in its mixture with diacrylate (DA) monomer has been determined by means of differential scanning calorimetry (DSC). PEO (T_m=65 °C), purchased from Scientific Polymer Products Inc., has a reported average molecular weight (M_w) of 66 000. 1,6-hexanediol diacrylate (T_m=10 °C) having a molecular weight of 226 was supplied by Aldrich Chemical Company and was used as received. Various concentrations of PEO were dissolved in diacrylate monomer by stirring for 15 h at 70 °C on a hot plate. For photopolymerization, Rose Bengal photoinitiator (1 wt % of reactive monomer) [22], with the aid of *N*-phenyl glycine (coinitiator), *N*-vinyl pyrrolidone (solubilizing agent), and octanoic acid (surfactant) were used [8,9].

The photocuring reaction was carried out using a photo-DSC (TA Instruments, Q-1000) under uv irradiation at 365 nm. Both the reference compartment containing empty pan and the sample holder containing PEO-DA mixtures (7.5 mg) were irradiated at an intensity of 150 mW/cm^2 at 70 °C for 10 min to ensure that all PEO crystals were melted before curing with ultraviolet light. To avoid possible influence of the residual solvent and thermal history, only the second runs were reported in the establishment of the relationship between melting temperatures versus concentration of PEO. The blend samples were heated in a hot stage (Limkam, TMS 93) under an optical microscope (Olympus, BX 60) at the desired experimental temperatures (i.e., above the melting points of each blend composition) for 10 min. The sandwiched samples were exposed to green light illuminated at 17 μW/cm^2 in order to trigger photopolymerization of DA in the mixtures. The emerged microsctures were photographed using a digital camera (Canon, EOS 300D) for various blends and isothermal reaction temperatures under a magnification of 50×.

III. MODEL DESCRIPTION

The present theory is an extension of the Flory-Huggins (FH) theory [23] of liquid-liquid demixing to the crystal solid–amorphous liquid phase separation by adding the crystal-amorphous interaction parameter [24] to the conven-

tional FH interaction parameter of segmental amorphous-amorphous interaction. The total free energy density of mixing of such crystal-amorphous polymer blends consists of the free energy density pertaining to the crystal order parameter of the crystalline constituent weighted by its volume fraction (ϕ) and the FH free energy of liquid-liquid demixing, viz. [24],

$$f(\psi_i,\phi) = \phi f(\psi_1) + (1-\phi) f(\psi_2) + \frac{\phi}{r_1}\ln(\phi) + \frac{(1-\phi)}{r_2}\ln(1-\phi) + \{\chi_{aa} + \chi_{ca}\psi_1^2 - \chi_{cc}\psi_1\psi_2 + \chi_{ac}\psi_2^2\}\phi(1-\phi). \quad (1)$$

Here χ_{aa} is the FH interaction parameter representing the amorphous-amorphous interaction of the constituent chains in the isotropic melt; it can be given in the form $\chi_{aa}=A+B/T$, where $A=0$ and $B=0.87$. χ_{ca} represents the repulsive crystal-amorphous interaction parameter. Note that the subscripts denote the constituent 1 (crystal) and constituent 2 (photoreactive monomer). r_1 and r_2 correspond to the statistical segmental lengths of the respective components. If photopolymerization is initiated in the blend, r_2 must be treated as the reaction time or as conversion dependent, i.e., $r_2(t)$.

To clarify the physical essence of the enthalpic contribution, Eq. (1) may be rewritten as

$$f(\psi_1,\phi) = \phi f(\psi_1) + \frac{\phi}{r_1}\ln(\phi) + \frac{(1-\phi)}{r_2}\ln(1-\phi) + \chi_{aa}\phi(1-\phi) + \chi_{ca}(\phi\psi_1)[(1-\phi)\psi_1] - \chi_{cc}(\phi\psi_1)[(1-\phi)\psi_2] + \chi_{ac}[(1-\phi)\psi_2](\phi\psi_2) \quad (2)$$

where the crystal phase order parameter ψ_1 can be defined as the ratio of the lamellar thickness l_1 of the first constituent to the lamellar thickness of a perfect crystal l_1^0, i.e., $\psi_1=l_1/l_1^0$, and thus it represents the linear crystallinity (i.e., one-dimensional crystallinity) of the crystallizing component [24–26]. Then the product of ϕ and ψ_1 in the last term of Eq. (1) corresponds to the bulk crystallinity of constituent 1 in the blend, whereas the product of $(1-\phi)$ and ψ_1 implies the amount of amorphous material interacting with the crystalline phase, and hence the last term $\chi_{ca}\phi\psi_1(1-\phi)\psi_1$ signifies the repulsive crystal-amorphous interaction. The same argument applies to the second crystalline constituent. In the case of cocrystals, the terms $(\phi\psi_1)$ and $[(1-\phi)\psi_2]$ represent the crystallinity of each crystalline constituent, and χ_{cc}, representing the strength of crystal-crystal interaction within the cocrystals may be expressed according to their geometric means, i.e., $\chi_{cc}=c_\omega\sqrt{\chi_{ca}\chi_{ac}}$, where $c_\omega=1$ signifies the ideal case and $c_\omega=0$ indicates complete immiscibility between crystalline phases, forming separate crystals, viz., χ_{ca} and χ_{ac} may be treated as independent [24]. Since the cocrystals are difficult to form in most crystalline polymer blends, the crystal-crystal interaction term may simply be dropped from Eq. (1) as in the present case.

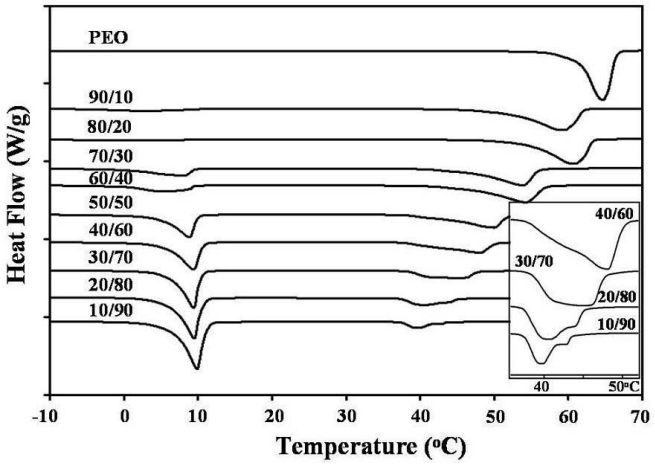

FIG. 1. DSC thermograms of PEO-DA blends obtained at a heating rate of 2 °C/min, showing a systematic movement of the melting peaks of PEO and DA as a function of concentration. The inset represents the enlarged dual melting peaks of PEO crystals in the blends.

The aforementioned crystal order parameter ψ may be described in the context of the phase field [22–25,27–29] based on a Landau-type free energy expansion [21,23,27], viz.,

$$f(\psi_i) = \frac{F(\psi_i)}{k_B T} = W_i\left(\frac{\zeta_i(T)\zeta_{i,0}(T_{m,i})}{2}\psi_i^2 - \frac{\zeta_i(T)+\zeta_{i,0}(T_{m,i})}{3}\psi_i^3 + \frac{1}{4}\psi_i^4\right), \quad (3)$$

where the subscript i represents each constituent. The coefficients of the Landau free energy expansion are treated as temperature dependent so that the free energy has the form of an asymmetric double well at a given crystallization temperature or supercooling; but it reverts to the symmetric double well at equilibrium. It should be cautioned that the coefficient of the third-order term must be nonzero in order to apply the Landau potential to the first-order phase transition [25,26]; otherwise, Eq. (3) is applicable only to a second-order phase transition or equilibrium. The parameter ζ represents the unstable hump for the crystal nucleation and W is the coefficient that represents the penalty to overcome the energy barrier for the nucleation process. ζ_0 represents the crystal order parameter at the solidification potential of crystallization, which is treated as crystal melting temperature dependent.

IV. RESULTS AND DISCUSSION

Figure 1 exhibits the DSC thermograms of PEO-DA blends obtained at a heating rate of 2 °C/min, showing the melting transition of neat PEO in the vicinity of $T_{m1}=65$ °C. This melting transition shows a systematic shift to a lower temperature with increasing DA content. The observed downward trend of the melting point of PEO with increasing DA content is consistent with those reported for other miscible or partially miscible blends [27–29] except that there appear dual melting peaks of PEO in the thermograms at low

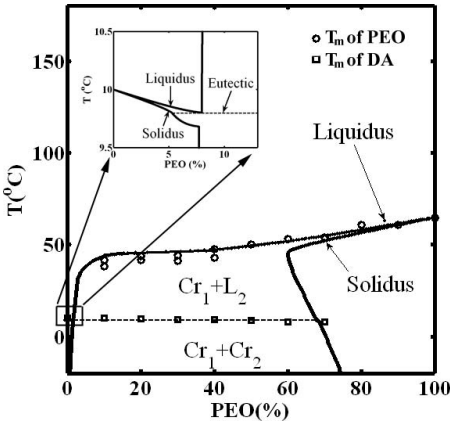

FIG. 2. Comparison between self-consistent solution (solid lines) and experimental melting temperatures of PEO-DA blends not containing any photocuratives, showing the crystal solid-liquid coexistence region bounded by the liquidus and solidus lines. The dashed eutectic line was drawn to demarcate Cr_1+L_2 and Cr_1+Cr_2 coexistence regions. The inset shows an enlarged view of the crystal transition close to the melting point of the monomer. Subscripts 1 and 2 indicate PEO and DA monomer, respectively. The parameters used were $r_1=10$, $r_2=1$, $\chi_{ca}=0.17$, $\chi_{ac}=0.01$, $\chi_{aa}=0.87$ at 40 °C, $\zeta_{01}=1$, $\zeta_{02}=1$, $T_{m1}=65$ °C, and $T_{m2}=10$ °C.

PEO concentrations. Such dual peaks are evident in the enlarged scale shown in the inset. Similar dual melting peaks were observed by Kerridge in the phase diagrams of binary triglyceride blends [30]. Concurrently, the melting peak of the neat DA is located at approximately $T_{m2}=10$ °C, which shows a very minor movement with increasing PEO content. At some concentrations, dual isotherms of DA can be seen if expanded. In view of the nonequilibrium nature of these melting peaks, additional DSC runs were performed at 5 and 10 °C/min, which further confirmed that these dual peaks at low PEO concentrations are reproducible. As depicted in Fig. 2, the self-consistent solution reveals a solid-liquid coexistence gap bounded by the solidus and liquidus lines. To demonstrate the role of the crystal-amorphous interaction in the phase diagram, the critical interaction parameter was taken as the FH interaction parameter $\chi_{aa}=0.87$ at the critical temperature of 40 °C along with the crystal-amorphous interaction parameter $\chi_{ca}=0.17$, the amorphous-crystal interaction parameter $\chi_{ac}=0.01$, $r_1=10$, $r_2=1$, $T_{m1}=65$ °C, $T_{m2}=10$ °C, $\zeta_{01}=1$, and $\zeta_{02}=1$. The close resemblance of the predicted trends of the solidus and liquidus lines to the experimental melting transition points indicates that the observed dual DSC peaks are real and can be attributed to the solidus and liquidus phases. The DA melting transitions show the coexistence of solidus and liquidus lines as well, but they are seemingly overlapped. These solidus and liquidus lines are clearly distinguishable in the eanlarged version shown in the inset of Fig. 2, along with the eutectic line. The present predicted trends are consistent with those in other binary systems, such as metal alloys or liquid crystalline mixtures; this might remedy the deficiency of the original Flory diluent theory [27,23], which predicts only a single liquidus line.

The addition of the photoinitiator to the mixture, when it was kept in the dark, further lowers the melting points of the

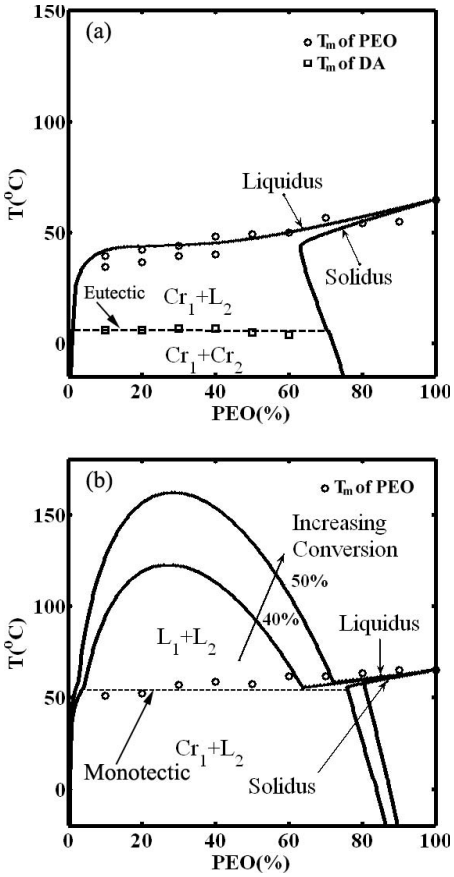

FIG. 3. (a) Calculated phase diagram in comparison with the DSC melting temperature of PEO and DA, showing crystal-liquid and crystal-crystal coexistence regions bounded by the liquidus and solidus lines prior to curing. Dashed line representing eutectic is drawn to demarcate Cr_1+L_2 and Cr_1+Cr_2 coexistence regions. (b) Theoretically calculated snapshots of increment of the UCST with increasing conversion in comparison with the enhanced DSC melting points of PEO-DA after photocuring. The crystallization of DA was prevented due to network formation after photo-cross-linking. Dashed line representing monotectic was drawn to demarcate L_1+L_2 and Cr_1+L_2 coexistence regions. Subscripts 1 and 2 indicate PEO and DA monomer, respectively.

PEO crystals [Fig. 3(a)] and also there is an identifiable liquid-liquid phase separated gap in the vicinity of the PEO crystal melting temperature. Assuming the diacrylate and photoinitator syrup are miscible and ignoring the polydispersity of PEO, the solidus and liquidus lines of this pseudobinary system can be determined by the aforementioned self-consistent approach. The dashed line representing the eutectic was drawn to demarcate the Cr_1+L_2 and Cr_1+Cr_2 regions, where Cr and L stand for crystal and liquid of the constituents, respectively.

When these mixtures are exposed to the uv light in the photo-DSC cell operated at a power of 150 mW/cm^2 at 70 °C for 10 min, photopolymerization of DA takes place in its PEO blends. As expected, liquid-liquid phase separation takes place, as signified by the snapshots of the temporal evolution of the upper critical solution temperature (UCST), which can be attributed to the increasing molecular weight or the conversion of the DA. By the same token, the melting

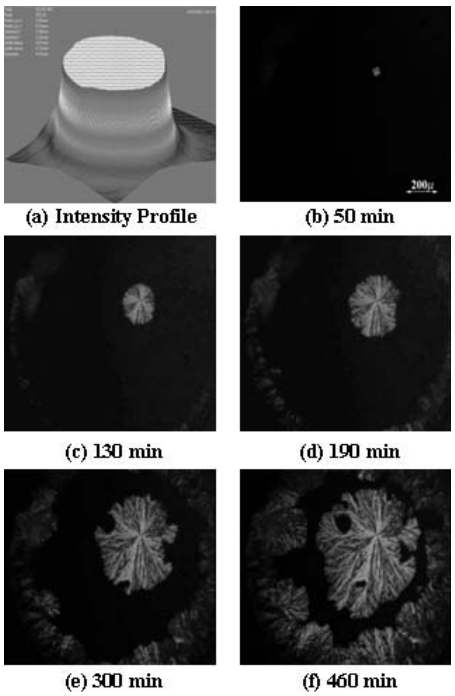

FIG. 4. (a) Intensity profile created using Iris diaphragm. (b)–(f) Time sequence of directional crystal growth of PEO showing the spherulitic growth at the core and epitaxial lamellar growth from the outer peripheral edge due to photopolymerization-induced crystallization. The cavities in the spherulite indicate pockets of trapped polymeric solvent. The scale bar represents 200 micrometer.

transition temperatures of PEO in the cured blends appreciably shift upward beyond the melting temperatures of the starting uncured blends [denoted by circles in Fig. 3(b)]. When the liquidus line surpasses the reaction temperature, crystallization commences, which is evidently induced by photopolymerization. That is to say, the increase in molecular weight of polyacrylate drives not only the UCST curve to move up, but also the melting point curve to surpass the reaction temperature, thereby thrusting the system into the unstable solid-liquid region, which in turn induces both phase separation and crystallization [24]. The lack of the DA melting peak in the cured blend may be attributed to the formation of DA networks during photocuring in the isotropic melt state, which prevented the crystallization of DA. The dashed line representing the monotectic is drawn to demarcate L_1+L_2 and Cr_1+L_2. To mimic the solidification of the PEO crystals, the 30:70 PEO-DA blends were illuminated with a green-filtered light intensity gradient in the optical microscope; it has a truncated Gaussian beam profile, in which the outer periphery has a lower intensity distribution relative to the truncated core region, which appeared uniform [Fig. 4(a)]. It can be anticipated that phase separation takes place where the reactive DA monomer diffuses to the high-intensity region whereas the nonreactive PEO molecules diffuse to the low-intensity circumference region where crystallization of PEO is expected to occur. When such a spatially nonuniform incident beam is utilized, directional solidification occurs by virtue of light intensity gradient at the circumference of the beam during photoreaction. Figures 4(b)–4(f) show the time sequence of the growth of PEO crystals when exposed to green light and examined under the optical microscope. It is not surprising for the crystal to nucleate early in the core region as compared to the circumference. The directional seaweed growth [25,26,31] occurs at the circumference, propagating toward the core. After some elapsed reaction time, spherulitic and epitaxial lamella, similar to the seaweed, branch out from the circumference and eventually transform into incomplete spherulites, thereby forming the grain boundaries between neighboring grains. The observed spherulites are reminiscent of the dense-branched morphology found in small-molecule systems [16–20] as well as some polymer spherulites [26,31]. At a first glance, this observation appears counterintuitive. However, after careful perusal, it seems plausible that phase separation takes place first in the mixture and drives the DA monomer and PEO chains to diffuse to the high- and low-intensity regions, respectively. The reaction occurring in the high-intensity region can locally drive the crystallization of PEO, because the melting point curve of the cured system is higher in this PEO-lean region, and thus PEO crystallization is feasible. On the other hand, the reaction in the PEO-rich region may not be fast enough to raise the originally depressed melting points. Consequently, it takes more time for the PEO-rich concentration to move from the isotropic melt state, and then it has to cross over the melting transition line before crystallization could take place. As a result, the predominance of the spherulitic growth in the high-intensity core region can be witnessed experimentally. Another interesting observation is the presence of polymeric solvent trapped in the emerged spherulite. The aforementioned directional crystal growth was verified in other isothermal photopolymerization-induced crystallization experiments on 10:90, 40:60, and 50:50 PEO-DA blends subjected to the truncated Gaussian intensity profile of the light intensity gradient (data not shown). It should be emphasized that the epitaxial growth of degeneracy or seaweed from the outer circumference presents experimental evidence of directional crystal growth driven by a photointensity gradient. The observed phenomenon is conceptually analogous to the directional crystal growth governed by a thermal gradient in small-molecule systems such as metal alloys [17–19], succinonitrile [20], and polymer crystallization [26,31]. Moreover, photopolymerization-induced phase transitions not only play a pivotal role in photolithography, three-dimensional photonic crystals, and holographic polymer-dispersed liquid crystals, but also represent one of the most vibrant fields with potential applications in organic and polymeric band gap materials and semiconductor technology [32].

V. SUMMARY

In summary, we have demonstrated experimentally that photopolymerization-induced crystallization takes place in blends of PEO-DA at temperatures above the depressed melting temperature of PEO. Although the photopolymerization was carried out at a constant temperature, the supercooling increases with progression of the reaction. Thus crystallization induced due to photopolymerization is analogous to

the nonisothermal gradual cooling case. The present paper elucidates various directionally solidified interface morphologies of polymer crystals subjected to a photointensity gradient. The knowledge of directional crystal growth thus acquired is of paramount importance in taking control of directional solidification processes such as photolithography and chemical deposition, among others, through use of light. Polymerization-induced phase transitions are interdisciplinary in nature because these underlying nonequilibrium and nonlinear processes share common ground with the directional solidification of metal alloys, ceramic mixtures, and excitable biological systems.

ACKNOWLEDGMENTS

Support of this work by the National Science Foundation through Grant No. DMR 0514942 is gratefully acknowledged. The authors express their gratitude to R. A. Matkar for his assistance in calculating the phase diagrams.

[1] J. Y. Kim, C. H. Cho, P. Palffy-Muhoray, M. Mustafa, and T. Kyu, Phys. Rev. Lett. **71**, 2232 (1993).
[2] T. Kyu and J.-H. Lee, Phys. Rev. Lett. **76**, 3746 (1996).
[3] X. Y. Wang, Y. K. Yu, and P. L. Taylor, J. Appl. Phys. **80**, 3285 (1996).
[4] H. Boots, J. Kloosterboer, C. Serbutoviez, and F. Touwslager, Macromolecules **29**, 7683 (1996).
[5] J. C. Lee, Phys. Rev. E **60**, 1930 (1999).
[6] D. Nwabunma, H. W. Chiu, and T. Kyu, J. Chem. Phys. **113**, 6429 (2000).
[7] T. Kyu and H. W. Chiu, Polymer **42**, 9173 (2001).
[8] V. P. Tondiglia, L. V. Natarajan, S. L. Sutherland, and T. J. Bunning, Adv. Mater. (Weinheim, Ger.) **14**, 187 (2002).
[9] S. Meng, T. Kyu, L. Natarajan, V. Tondiglia, R. Sutherland, and T. Bunning, Macromolecules **38**, 4844 (2005).
[10] H. Tanaka and T. Nishi, Phys. Rev. Lett. **55**, 1102 (1985).
[11] H. Tanaka and T. Nishi, Phys. Rev. A **39**, 783 (1989).
[12] H. Wang, K. Shimizu, E. K. Hobbie, Z. Wang, and C. C. Han, J. Chem. Phys. **116**, 7311 (2002).
[13] H. Wang, K. Shimizu, E. K. Hobbie, Z.-G. Wang, J. C. Meredith, A. Karim, E. J. Amis, B. S. Hsiao, E. T. Hsieh, and C. C. Han, Macromolecules **35**, 1072 (2002).
[14] J. D. Gunton, M. SanMigueal, and S. P. Sahni, in *Phase Transitions and Critical Phenomena*, edited by C. Domb and J. L. Lebowitz (Academic Press, New York, 1983), p. 267.
[15] J. S. Langer, in *Directions in Condensed Matter Physics*, edited by G. Grinstein and G. Mazenko (World Scientific, Philadephia, 1986), p. 165.
[16] G. Caginalp and P. Fife, Phys. Rev. B **33**, 7792 (1986).
[17] R. Kobayashi, Physica D **63**, 410 (1993),.
[18] S. Akamatsu, G. Faivre, and T. Ihle, Phys. Rev. E **51**, 4751 (1995).
[19] V. Ferreiro, J. F. Douglas, J. A. Warren, and A. Karim, Phys. Rev. E **65**, 042802 (2002).
[20] T. M. Guo, H. Xu, T. Kyu, and G. X. Wang, in *Solidification Processes and Microstructures*, edited by M. Rappaz, C. Beckermann, and R. Trivedi (TMS, Warrendale, PA, 2004), p. 393.
[21] A. V. Holden, M. Marcus, and H. G. Othmer, *Nonlinear Wave Processes in Excitable Media* (Plenum Press, New York, 1991).
[22] O. Valdes-Aguilera, C. Pathak, J. Shi, D. Watson, and D. Neckers, Macromolecules **25**, 541 (1992).
[23] P. J. Flory, *Principles of Polymer Chemistry* (Cornell University Press, Ithaca, NY, 1953).
[24] R. Matkar and T. Kyu, J. Phys. Chem. B **110**, 12728 (2006).
[25] H. Xu, R. Matkar, and T. Kyu, Phys. Rev. E **72**, 011804 (2005).
[26] H. Xu, W. Keawwattana, and T. Kyu, J. Chem. Phys. **123**, 124908 (2005).
[27] T. Nishi and T. Wang, Macromolecules **8**, 909 (1975).
[28] P. Smith and J. Manley, Macromolecules **12**, 483 (1979).
[29] Z. Qiu, T. Ikehara, and T. Nishi, Polymer **44**, 2799 (2003).
[30] R. Kerridge, J. Chem. Soc. (**1952**) 4577.
[31] L. Granasy, T. Pusztai, T. Borzsonyi, J. A. Warren, and J. F. Douglas, Nat. Mater. **3**, 645 (2004).
[32] P. N. Prasad, *Nanophotonics* (Wiley Interscience, Hoboken, NJ, 2004).